Catena 160 (2018) 385–393

Contents lists available at ScienceDirect

Catena

journal homepage: www.elsevier.com/locate/catena

Estimating the spatial relationships between soil hydraulic properties and soil physical properties in the critical zone (0–100 m) on the Loess Plateau, China: A state-space modeling approach

Jiangbo Qiao[a], Yuanjun Zhu[b], Xiaoxu Jia[c], Laiming Huang[c], Ming'an Shao[b,c,*]

[a] College of Resources and Environment, Northwest A & F University, Yangling 712100, China
[b] State Key Laboratory of Soil Erosion and Dryland Agriculture on the Loess Plateau, Northwest A & F University, Yangling 712100, China
[c] Key Laboratory of Ecosystem Network Observation and Modeling, Institute of Geographic Sciences and Natural Resources Research, Chinese Academy of Sciences, Beijing 100101, China

ARTICLE INFO

Keywords:
Earth's critical zone
Linear regression
Soil hydraulic properties
Spatial variation
State-space model

ABSTRACT

Soil hydraulic properties (SHP) such as the soil water retention curve and soil saturated hydraulic conductivity (Ks) of the deep profile in the Earth's critical zone (CZ) are important factors for investigating the water cycle process in the CZ. However, details are lacking about the SHP for the deep profile as well as their relationships with other soil properties. In the present study, SHP were obtained for a 100-m profile by soil core drilling, where the objectives were to understand the spatial distributions of SHP and to quantify the relationships between SHP and soil properties based on state-space model analysis and linear regression analysis. The results showed that SHP were not significantly related to the silt content and there was no cross-correlation between SHP and the soil organic carbon content. The soil physical properties (bulk density, sand content, and clay content) could account for most of the total variation in SHP. Compared with linear regression analysis, state-space modeling described the spatial relationship between SHP and soil physical properties much better. This study provides information about the SHP in deep profiles, thereby provide important parameters for investigating the water cycling process in the CZ and for developing pedotransfer functions.

1. Introduction

The Earth's critical zone (CZ) is the intersection area for matter migration and energy exchange in the pedosphere, atmosphere, hydrosphere, biosphere, and lithosphere in terrestrial ecosystems (National Research Council, 2001), and thus it is the key area for sustaining ecosystem functioning and human survival (Lin, 2010). Water cycle processes form the core center of matter cycling in the Earth's CZ, so it is helpful to understand the interactions between vegetation and water cycle processes.

Soil hydraulic properties (SHP) are key factors for understanding and describing the migration of water and chemical materials in the soil (Strudley et al., 2008) because they influence and control the migration and distribution of soil water (Horn, 2004; Strock et al., 2001). Thus, it is important to study the SHP to understand water cycle processes in the Earth's CZ. The SHP mainly comprise the soil water retention curve (SWRC), which describes the relationship between the soil water content and soil water potential, and the soil saturated hydraulic conductivity (Ks), which is an important physical property that influences soil water movements and solute transport (Buttle and House, 1997; Mallants et al., 1997). In addition, understanding the spatial distributions of SHP and the relationship between SHP and related factors is necessary for modeling soil water dynamics and developing pedotransfer functions for SHP.

Previous studies have determined the spatial distributions of SHP and the relationships between SHP and related factors mainly in shallow layers (0–5 m) (Kai-Hua et al., 2011; Lai and Ren, 2016; Liu et al., 2007; She et al., 2017). For example, the spatial distributions in the hydraulic properties of a multi-layered soil profile (0.1, 0.5, and 0.9 m) were investigated by Mallants et al. (1996). Sobieraj et al. (2002) estimated the spatial distributions of Ks along a tropical rainforest *catena* (20, 30, 50, and 90 cm). Biswas and Si (2009) studied the spatial relationship between SHP and related soil physical properties in farmland. Wang et al. (2015) estimated the relationship between the Van Genuchten (VG) soil parameters and soil properties as well as environmental factors on the Loess Plateau (0–5 cm). In addition, Lai and Ren (2016) proposed three inverse modeling approaches for estimating the effective hydraulic parameters in heterogeneous soils at the field

* Corresponding author.
E-mail addresses: jiangboqiao815@163.com (J. Qiao), shaoma@igsnrr.ac.cn (M. Shao).

http://dx.doi.org/10.1016/j.catena.2017.10.006
Received 12 March 2017; Received in revised form 22 September 2017; Accepted 3 October 2017
Available online 13 October 2017

scale. She et al. (2017) examined the multi-scale correlations between SHP and soil factors as well as topographic attributes by multivariate empirical mode decomposition along a Brazilian watershed transect (0–0.2 m). Bevington et al. (2016) investigated the scale dependencies of SHP by factorial kriging analysis in Holocene coastal farmland (8–68 cm).

Clearly, the relationships between SHP and other factors in shallow layers (0–5 m) have been studied widely from different perspectives. However, the vertical distance of the Earth's CZ ranges from the top of the plant canopy to the weathered bedrock (Lin, 2010), but insufficient information is available about SHP to investigate water processes in the Earth's CZ (> 5 m). Therefore, there is an urgent need to determine the spatial distributions in the SHP of deep soil layers and to investigate the relationships between SHP and other soil properties.

In addition, many methods have been employed to estimate the relationships between variables and correlated variables, such as linear regression and state-space modeling. Linear regression modeling ignores the coordinates and spatial correlation (Goovaerts, 1999), whereas state-space modeling considers the spatial dependences between variables. Several studies have concluded that state-space modeling is a better tool for accurately estimating the relationships between variables and correlated factors (Jia et al., 2012; Liu et al., 2012; Wendroth et al., 2003). For example, Timm et al. (2004) evaluated the relationships between the physical and chemical properties of soil. In addition, She et al. (2014) and Liu et al. (2012) both estimated the soil organic carbon (SOC) contents based on topographic properties using a state-space model and showed that the state-space models performed better than the equivalent linear regression models. Similarly, Duan et al. (2016) concluded that state-space models are much better for describing the spatial patterns of soil water storage. Jia et al. (2011) estimated the relationship between the total net primary productivity by managed grasslands and soil properties using a state-space model approach.

Therefore, the objectives of this study were: (i) to determine the spatial distributions of SHP and quantify the relationships between SHP and other soil properties, i.e., the bulk density (BD) and sand, silt, clay, and SOC contents, by a state-space model along a deep profile (0–100 m) in the Earth's CZ; and (ii) to compare the results obtained by state-space modeling and linear regression analysis.

2. Materials and methods

2.1. Study area description

The study was conducted at Changwu station of the Chinese Academy of Sciences, which is located on the Loess Plateau of China (N35°12′ N, E107°40′ E) (Fig. 1b). This area has a continental climate, where the mean annual precipitation is 580 mm and the mean annual temperature is 9.1 °C. The ground water level is 50–80 m. The soil texture is silt loam and the soil type is dark loessial soil, where the parent material is deep loamy Malan loess. The geomorphic landform belongs to the typical plateau tableland region and typical dry rain-fed agriculture is conducted in this area. The deep soil layer and good physical properties provide favorable conditions for plant growth, and agricultural production and ecological environment construction are prominent in this area.

2.2. Soil sampling

Soil samples were collected using drilling equipment (assembled by Xi'an Qinyan Drilling Co., LDT). Metal cylinders (diameter: 5 cm, length: 5 cm) were used to collect undisturbed soil samples in the middle of the soil column at 1-m intervals (0.5 m, 1.5 m, 2.5 m, 3.5 m, …) to obtain measurements of the Ks, SWRC, and BD. Similarly, disturbed soil samples were collected to determine the soil particle composition and soil organic matter contents. It should be noted that the undisturbed soil samples were not replicated due to cost and challenges obtaining the samples. Finally, the drilling depth is 204.5 m and 204 undisturbed soil cores and 204 disturbed soil samples were collected and the sample collection process was completed in a period of 10 days (May 17–27, 2016). It is noted that it is difficult to measure SHP of undisturbed soil samples after 100 m. Therefore, we attained the data of SHP from 0 to 100 m.

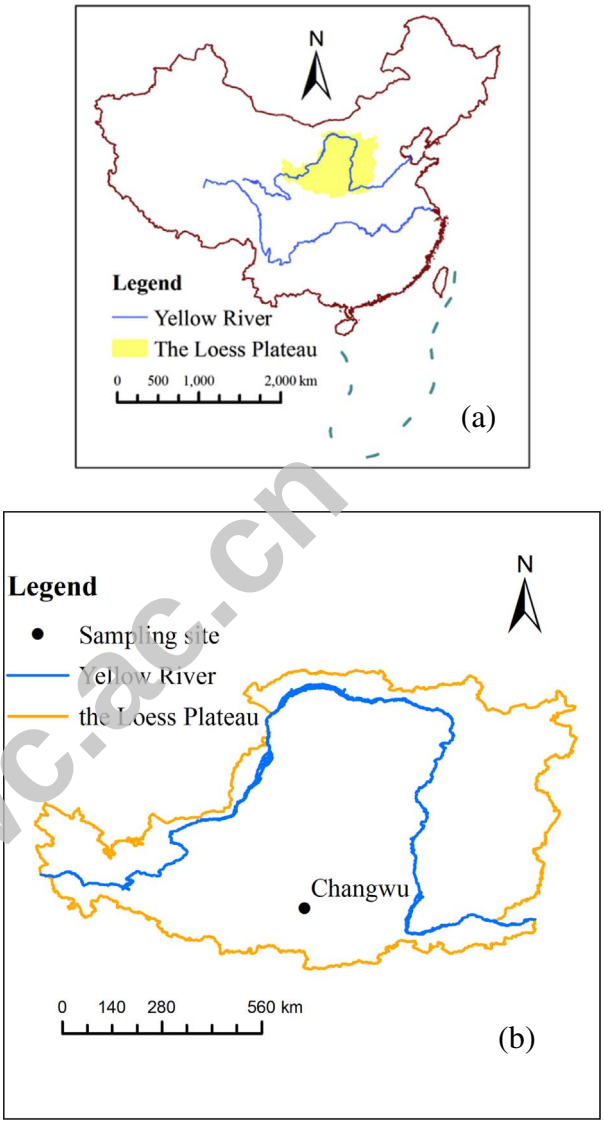

Fig. 1. Location of the Loess Plateau region in China (a) and the sampling site (b).

2.3. Laboratory analysis

Ks was determined for undisturbed soil samples using the constant head method (Wang et al., 2008), SWRC was measured by the centrifugation method (Hitachi CR21G centrifuge; 20 °C) (Lu et al., 2004), and BD was determined based on the volume–mass relationship for each oven-dried core sample (Wang et al., 2008). The disturbed soil samples were also air-dried and passed through a 1.0-mm mesh, before measuring the soil particle composition by laser diffraction (Mastersizer 2000, Malvern Instruments, Malvern, England) (Liu et al., 2005), and through a 0.25-mm mesh to determine the SOC by dichromate oxidation (Nelson & Sommers, 1982).

2.4. Fitting the SWRC

Many models have been developed to fit the SWRC and the VG model is one of the most commonly models (Liu et al., 2007). Therefore, the VG equation (Genuchten, 1980) was used to fit the measured SWRC data. The equation for the VG model (Genuchten, 1980) is:

$$\theta(h) = \theta r + \frac{(\theta s - \theta r)}{(1 + |\alpha h|^{n})^{1-\left(\frac{1}{n}\right)}} \quad (1)$$

where θ(h) is the volumetric water content ($cm^3\ cm^{-3}$) for the soil water pressure head h (cm), θs is the saturated soil water content ($cm^3\ cm^{-3}$), θr is the residual soil water content ($cm^3\ cm^{-3}$), α is a fitting parameter related to the inverse of the air entry pressure, and n is a fitting parameter related to the soil pore distribution.

2.5. Theory of state-space modeling

The state-space model comprises a state equation and observation equation, which describe how the state of one or more variables at location i are correlated with the state of other variables at location i − 1 (Nielsen et al., 1999; Shumway et al., 1989). The state equation is described as follows:

$$X_i = \Phi x_{i-1} + w_i \quad (2)$$

where X_i is the state vector of several variables at location i, Φ is a p × p matrix of state coefficients, and w_i is the model error vector (Timm et al., 2003). The model error, which is assumed to be uncorrelated, is a zero valued and normally distributed noise with an m ∗ m covariance matrix Q, where the latter is the variance per unit space and it depends on the interval between observations.

The observation equation is formed by the contact between the state vector (X_i) and observation vector (Y_i), and it is described as:

$$Y_i = A_i X_i + v_i \quad (3)$$

where the observation vector, Y_i, is associated with the state vector X_i through the observation matrix A_i and model error, v_i, which is also considered to be zero, uncorrelated, and normally distributed. However, v_i and w_i are assumed to be independent of each other. The observation vector, Y_i, cannot represent the whole real state and it is only an indirect reflection of the state (Jia et al., 2011; Jia et al., 2012). Both the state coefficient matrix, Φ, and state covariance matrix, Q, are evaluated by a recursive procedure (Shumway and Stoffer, 1982), and they are optimized using the Kalman filtering iteration procedure (Kalman, 1960).

In order to remove differences in magnitude, it is necessary to normalize the data before state-space analysis. The normalization equation is described as:

$$z_i = [Z_i - (m - 2s)]/(4s) \quad (4)$$

where z_i is the normalized value with a mean of 0.5 and standard deviation of 0.25 (Wendroth et al., 1999), m is the mean value, and s is the standard deviation.

2.6. Statistical analysis

Descriptive statistical analyses (including the maximum, minimum, average, coefficient of variation (CV)), Pearson's correlation analysis, and linear regression analysis were performed with SPSS (version 16.0). Nonlinear regression of the SWRCs was conducted with RETC software (version 6.0). The autocorrelations and cross-correlations of variables and the state-space model were determined using applied statistical time series analysis (ASTSA), as developed by Shumway (1988).

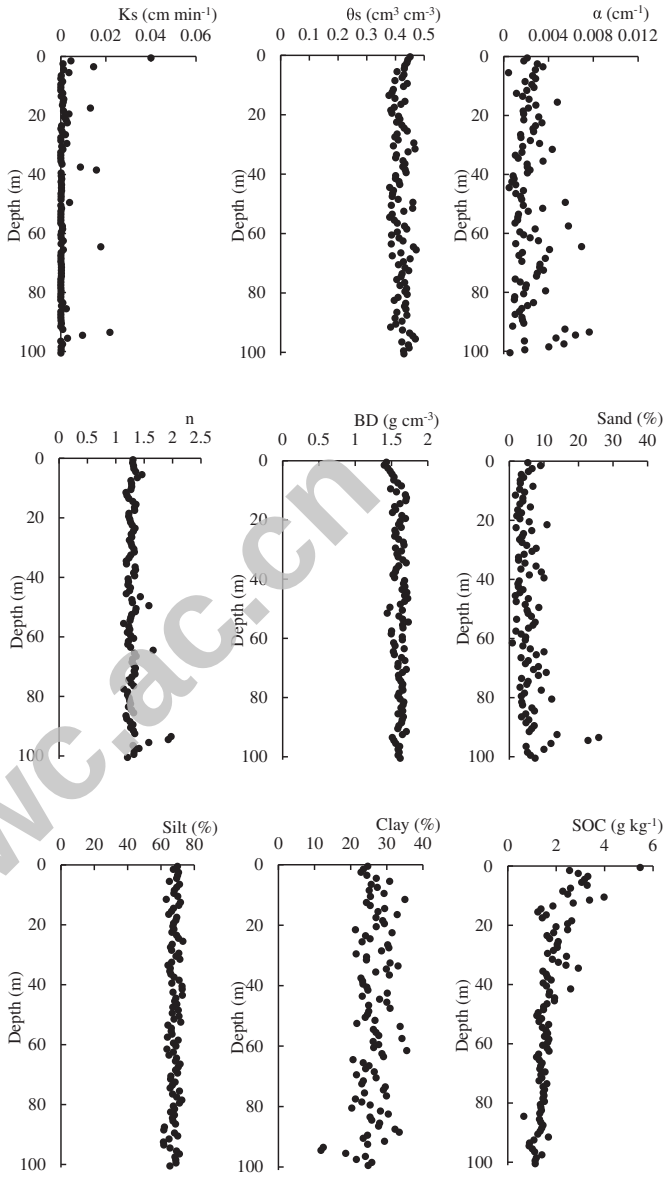

Fig. 2. Spatial distributions of soil hydraulic properties (SHP) and soil properties along the 100 m profile.

3. Results and discussion

3.1. Spatial distribution of SHP and their correlations with soil properties

Fig. 2 shows the spatial distributions of SHP along the profile. θs and n remained almost stable along the profile, with CV values of 5.58% and 9.48%, respectively (Table 1). The Ks values for SHP ranged from 1.0×10^{-6} to 0.04 cm min^{-1}, with strong variation (CV = 274.61%) (Nielsen and Bouma, 1985). This may be explained by the unique profile structure of the Loess Plateau, which was formed by 37 climate cycles and comprises different soil layers, thereby resulting in the strong variation in Ks (Ding et al., 1989). In addition, there was moderate variation in α throughout the profile (CV = 58.96%). Among the soil properties, silt and BD varied little, whereas the sand, clay, and SOC contents exhibited moderate variation.

Pearson's correlation analysis was conducted between SHP and other soil properties to select the variables used in the state-space analysis (Table 2). Given the deep profile, variables comprising sand, silt, clay, BD, and SOC were selected for Pearson's correlation analysis with SHP. The four hydraulic properties were all negatively correlated

Table 1
Descriptive statistics for the soil hydraulic properties (SHP) and basic soil properties.

Parameter	Min	Max	Mean	SD	CV	Skewness	Kurtosis
Ks, cm min^{-1}	0.000001	0.040	0.002	0.005	2.746	4.717	26.609
θs, cm^3 cm^{-3}	0.378	0.472	0.420	0.023	0.056	0.170	− 0.744
α, cm^{-1}	0.0004	0.008	0.002	0.001	0.590	1.466	2.396
n	1.138	1.974	1.301	0.123	0.095	3.365	14.884
Sand, %	0.888	25.862	5.707	3.700	0.648	2.820	11.854
Silt, %	61.479	73.126	67.962	2.611	0.038	− 0.296	− 0.188
Clay, %	11.789	35.536	26.331	4.028	0.153	− 0.486	1.937
BD, g cm^{-3}	1.400	1.732	1.605	0.071	0.044	− 0.587	− 0.065
SOC, g kg^{-1}	0.664	5.472	1.781	0.713	0.400	2.161	6.972

Min, minimum; Max, maximum; SD, standard deviation; CV, coefficient of variation; BD, bulk density; SOC, soil organic carbon.

Table 2
Pearson's correlation coefficients between soil hydraulic properties (SHP) and selected soil properties.

Parameter	Ks	θs	α	n	BD	Sand	Silt	Clay	SOC
Ks	1	0.282**	0.330**	0.451**	− 0.469**	0.341**	0.019	− 0.325**	0.349**
θs		1	0.647**	0.419**	− 0.704**	0.417**	0.09	− 0.441**	− 0.104
α			1	0.651**	− 0.508**	0.552**	− 0.136	− 0.419**	− 0.210*
n				1	− 0.380**	0.709**	− 0.12	− 0.573**	− 0.209*

* Correlation significant at $P < 0.05$ (two-tailed).
** Correlation significant at $P < 0.01$ (two-tailed).

with BD and the clay contents, but positively correlated with the sand contents ($P < 0.01$). All of the SHP were not related to the silt content, probably due to the low variation in the silt content (CV = 3.8%). In addition, Ks was significantly associated with SOC ($P < 0.01$), and α and n were negatively correlated with SOC ($P < 0.05$). We selected variables that had significant relationships with the SHP to conduct the state-space analysis. Therefore, the variables used for the state-space analysis of Ks, α, and n comprised BD and the sand, clay, and SOC contents, but the SOC content was not selected for θs.

3.2. Autocorrelation functions (ACFs) and cross-correlation functions (CCFs) between SHP and related variables

ACFs and CCFs were used to calculate the spatial correlations of different distances among variables, where the details of the ACF and CCF have been described in other studies (Timm et al., 2003). The variables must be significantly autocorrelated and cross-correlated with other variables in state-space analysis (Wendroth et al., 2003). At the 95% confidence level, Fig. 3 showed the ACFs for SHP and the soil properties. The results demonstrated that all the variables were autocorrelated according to the state-space analysis and SOC had a significant spatial autocorrelation up to 12 lags, whereas one or two lags were found for the other variables. This might be explained by the different loess-paleosol layers formed on the Loess Plateau by 37 climate cycles (Ding et al., 1989), thereby resulting in spatial autocorrelations with low lags between adjacent observations. The ACF results showed that the sampling density was sufficient to identify the spatial representativeness of the variables.

The spatial cross-correlations differed in various directions as well as the lags between SHP and related variables according to the results of the CCF analysis (Fig. 4). In particular, the hydraulic properties were all significantly cross-correlated with BD and the sand and clay contents, but there were no cross-correlations with SOC for Ks, α, and n (Fig. 4). Therefore, SOC was removed from the subsequent state-space analysis. The results obtained for the cross-correlation functions showed that it was possible for the selected variables to be used to assess SHP in the state-space analysis.

3.3. State-space model for SHP

The state-space model described the spatial distributions for the SHP and quantified the relationships between the SHP and other variables in the neighborhood. Table 3 shows the state-space equations for different combinations and their coefficient of determination (R^2) values.

For Ks, the best bivariate state-space model equation included clay with an R^2 value of 0.874, and the bivariate model including BD had a similar R^2 value ($R^2 = 0.870$). Among the trivariate models, the best included BD and clay contents, with an R^2 value of 0.855. The R^2 value for the multivariate equation including BD, sand contents, and clay contents was 0.757. Obviously, increasing the number of variables did not make the R^2 value increase. The state space model analyses for n, α, and θs obtained the same results, in a similar manner to previous studies (Jia et al., 2011; Liu et al., 2012). The clay content was considered to be the most important variable, where it explained 87.45% of the total variation and it was associated with the best performance. It should be noted that BD was also an important variable, where it explained 87% of the total variation. Zhao et al. (2014) estimated the Ks values for a slope on the northern Loess Plateau and also concluded that BD and soil particles were the key factors that affected Ks. Ks has a significant relationship with the soil porosity and soil texture, and BD and the clay contents also have major effects on the soil porosity and soil texture.

For θs, the best performance among the bivariate equations was for BD ($R^2 = 0.897$), and with BD and sand in the trivariate equation ($R^2 = 0.798$). It should be noted that the sand content only explained 33.6% of the total variation (Table 3), thereby suggesting that the sand content was not an important variable. Given its superior performance, BD was the most important variable with the highest R^2 value ($R^2 = 0.897$).

The best R^2 value obtained for α among the bivariate equations was 0.948, which included BD, and $R^2 = 0.966$ among the trivariate variables including BD and sand contents. The multivariate combination of BD, and clay and silt contents had an R^2 value of 0.965. The best models included BD and sand contents.

Compared with other SHP, the best model in terms of n had the highest R^2 value ($R^2 = 0.987$), which included the sand and clay contents. Obviously, soil texture was the most important for n, where it

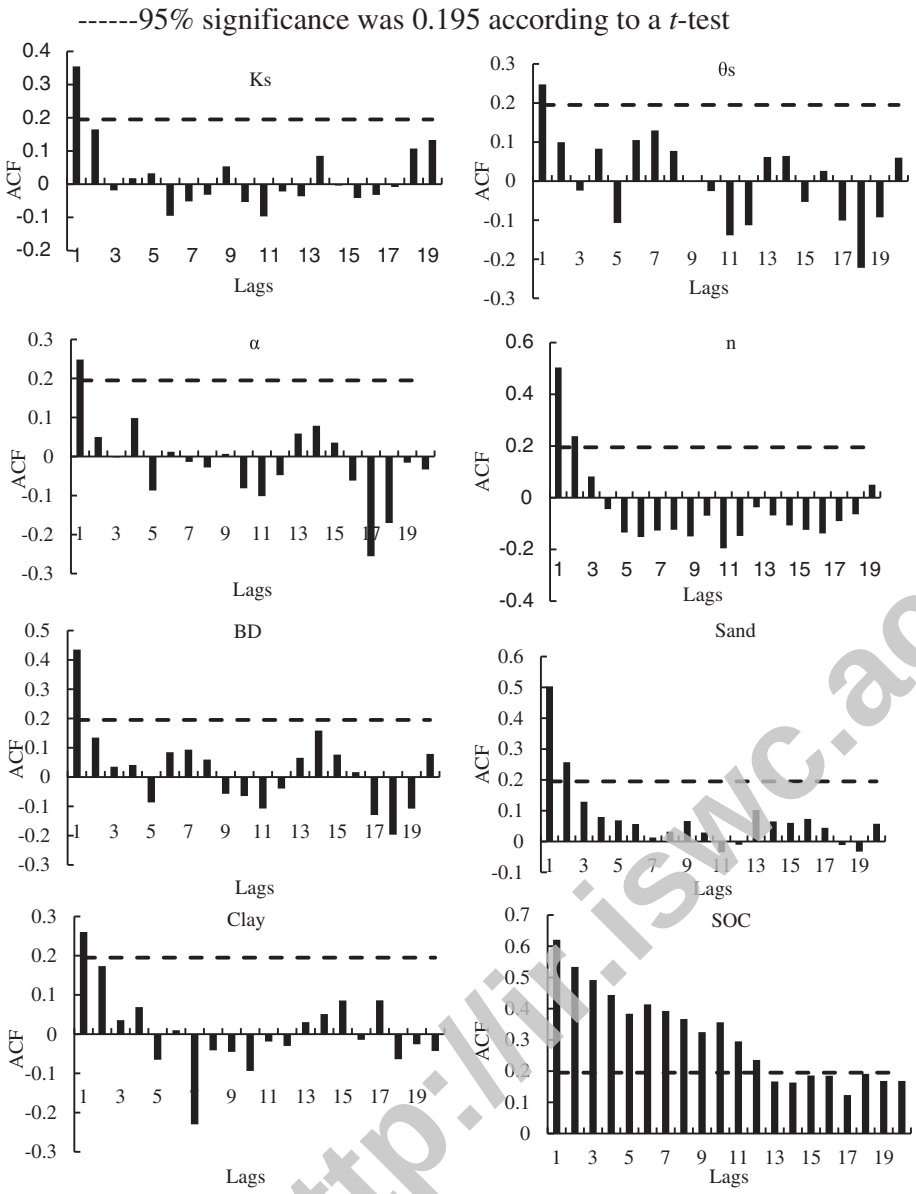

Fig. 3. Autocorrelation functions (ACF) for soil hydraulic properties (SHP) and related variables.

explained 0.987 of the total variation.

Clearly, BD was an important factor for all SHP, where it could explain 87.0%, 89.7%, 94.8%, and 91.2% of the total variations in Ks, θs, α, and n, respectively. Wang et al. (2015)) investigated the spatial variability of SWRC (VG model) on the Loess Plateau and also found that BD contributed greatly to the variations in the VG parameters (except for α). Moreover, Biswas and Si (2009) investigated the relationship between SHP and soil physical properties, and showed that BD was significantly correlated with the VG parameters (except for α) and Ks. BD is a basic soil physical property that can affect the transport of water and solutes, and it is an indicator of the soil quality and soil compaction, thereby making it an important variable for SHP.

In addition, the soil physical properties explained all the variations in SHP, whereas SOC was not an important factor among the soil chemical properties in terms of its contribution to variations in the SHP. This result is not consistent with those obtained in other studies. For example, Wang et al. (2015) analyzed the factors that affected the VG parameters and showed that SOC contributed greatly to the variations in the VG parameters (except for α). Fu et al. (2015) also analyzed the important factors for Ks in a small karst catchment and found that SOC was one of the most important factors. SOC is an important chemical property that is influenced by BD and the soil texture (Liu et al., 2012), thereby influencing the SHP. We found that the upper soil layers had higher SOC contents, which were affected by plant growth and human activities to influence the variations in the SHP. The SOC was low in the deep soil layer, so it had no effects on the variations in the SHP.

In order to evaluate the results, the state-space models with the best performance for every SHP were tested in two different scenarios (using all of the SHP measurements and 50% of the SHP measurements). Figs. 5–8 show the observed, estimated, and omitted SHP values, as well as the estimated 95% confidence intervals for the best performing models in different scenarios. The width of the 95% confidence interval represents ± 2 standard deviations for each estimated value at position i.

The coefficients of the same equations were different (Figs. 5–8), which indicates that the weights of the variables depended on the available data (Wendroth et al., 2001). For Ks, θs, and α, the R^2 values obtained by the state-space models using 50% of the data were similar to those using all the measured data, or even higher, whereas the R^2 values decreased for n. Liu et al. (2012) also reported that the state-space models for estimating SOC across a large-scale region performed better when using 50% of the data. However, Jia et al. (2011) estimated

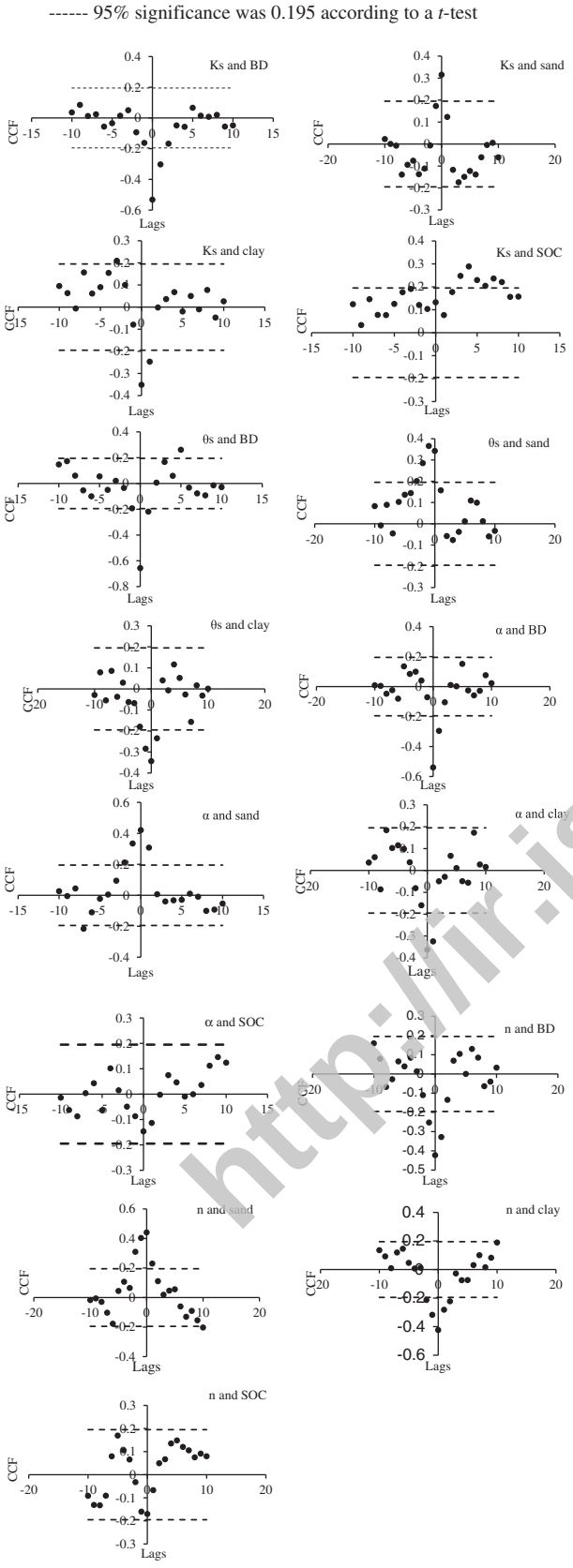

Fig. 4. Cross-correlation functions (CCF) for soil hydraulic properties (SHP) with the bulk density (BD), and sand, silt, clay and soil organic carbon (SOC) contents.

Table 3
State-space analysis of soil hydraulic properties (SHP) using the bulk density (BD), and sand and clay contents.

State-space model	R^2
$(Ks)_i = 0.768 * (Ks)_{i-1} + 0.237 * (BD)_{i-1} + w_i$	0.870
$(Ks)_i = 0.855 * (Ks)_{i-1} + 0.100 * (sand)_{i-1} + w_i$	0.724
$(Ks)_i = 0.760 * (Ks)_{i-1} + 0.229 * (clay)_{i-1} + w_i$	0.875
$(Ks)_i = 0.809 * (Ks)_{i-1} - 0.046 * (BD)_{i-1} + 0.247 * (sand)_{i-1} + w_i$	0.809
$(Ks)_i = 0.795 * (Ks)_{i-1} - 0.008 * (BD)_{i-1} + 0.221 * (clay)_{i-1} + w_i$	0.855
$(Ks)_i = 0.840 * (Ks)_{i-1} + 0.348 * (sand)_{i-1} - 0.179 * (clay)_{i-1} + w_i$	0.769
$(Ks)_i = 0.767 * (Ks)_{i-1} - 0.075 * (BD)_{i-1} + 0.023 * (sand)_{i-1} + 0.294 * (clay)_{i-1} + w_i$	0.757
$(\theta s)_i = 0.697 * (\theta s)_{i-1} + 0.321 * (BD)_{i-1} + w_i$	0.897
$(\theta s)_i = 0.501 * (\theta s)_{i-1} + 0.474 * (sand)_{i-1} + w_i$	0.336
$(\theta s)_i = 0.756 * (\theta s)_{i-1} + 0.238 * (clay)_{i-1} + w_i$	0.818
$(\theta s)_i = 0.825 * (\theta s)_{i-1} - 0.461 * (BD)_{i-1} + 0.660 * (sand)_{i-1} + w_i$	0.798
$(\theta s)_i = 0.655 * (\theta s)_{i-1} + 0.046 * (BD)_{i-1} + 0.321 * (clay)_{i-1} + w_i$	0.771
$(\theta s)_i = 0.809 * (\theta s)_{i-1} + 0.340 * (sand)_{i-1} - 0.140 * (clay)_{i-1} + w_i$	0.583
$(\theta s)_i = 1.136 * (\theta s)_{i-1} - 0.609 * (BD)_{i-1} - 0.420 * (sand)_{i-1} + 0.907 * (clay)_{i-1} + w_i$	0.751
$(\alpha)_i = 0.746 * (\alpha)_{i-1} + 4.318 * (BD)_{i-1} + w_i$	0.948
$(\alpha)_i = 0.966 * (\alpha)_{i-1} + 0.038 * (sand)_{i-1} + w_i$	0.906
$(\alpha)_i = 0.816 * (\alpha)_{i-1} + 3.020 * (clay)_{i-1} + w_i$	0.905
$(\alpha)_i = 0.736 * (\alpha)_{i-1} + 0.135 * (BD)_{i-1} + 2.099 * (sand)_{i-1} + w_i$	0.966
$(\alpha)_i = 0.664 * (\alpha)_{i-1} + 0.099 * (BD)_{i-1} + 4.10 * (clay)_{i-1} + w_i$	0.835
$(\alpha)_i = 0.708 * (\alpha)_{i-1} + 0.086 * (sand)_{i-1} + 0.261 * (clay)_{i-1} + w_i$	0.949
$(\alpha)_i = 0.658 * (\alpha)_{i-1} + 0.132 * (BD)_{i-1} + 0.187 * (sand)_{i-1} + 0.008 * (clay)_{i-1} + w_i$	0.965
$(n)_i = 0.777 * (n)_{i-1} + 0.176 * (BD)_{i-1} + w_i$	0.912
$(n)_i = 0.904 * (n)_{i-1} + 0.052 * (sand)_{i-1} + w_i$	0.981
$(n)_i = 0.860 * (n)_{i-1} + 0.138 * (clay)_{i-1} + w_i$	0.934
$(n)_i = 0.884 * (n)_{i-1} - 0.161 * (BD)_{i-1} + 0.290 * (sand)_{i-1} + w_i$	0.898
$(n)_i = 0.856 * (n)_{i-1} - 0.019 * (BD)_{i-1} + 0.177 * (clay)_{i-1} + w_i$	0.899
$(n)_i = 0.711 * (n)_{i-1} + 0.289 * (sand)_{i-1} + 0.008 * (clay)_{i-1} + w_i$	0.987
$(n)_i = 0.932 * (n)_{i-1} - 0.194 * (BD)_{i-1} - 0.069 * (sand) + 0.343 * (clay)_{i-1} + w_i$	0.846

the total net primary productivity of managed grasslands by state-space modeling and concluded that the R^2 values were lower when using 50% of data. It is possible that the different variables used in diverse areas had different spatial correlations with other variables and the data available.

In addition, the width of the 95% confidence interval was even narrower for n when using 50% of the data (Fig. 8) and the R^2 values decreased, which is not consistent with the results obtained in other studies (She et al., 2014; Wendroth et al., 2003), where the 95% confidence interval was narrower so the predictions were more accurate. The omission of some extremely high and low values might explain these results (Fig. 8b).

3.4. Comparison of state-space analysis and linear regression analysis

The linear regression analysis results for different combinations of the SHP are shown in Table 4. It should be noted that the variables were tested for normality and log-transformation was necessary for variables that differed from normality. The variables related to the best performance for the SHP were similar to those determined by the state-space analysis (except for Ks). The R^2 values for the best models according to linear regression analysis were 0.312, 0.564, 0.375, and 0.292 for Ks, θs, α, and n, respectively, and 0.875, 0.897, 0.966, and 0.987 by state-space modeling. Thus, all the R^2 values for different combinations according to state-space analysis were slightly higher than those using the equivalent linear regression equations. Therefore, the state-space models described the spatial patterns of the variables better, which may be explained by the consideration of the spatial variability among the SHP and other variables in the state-space model.

4. Conclusion

Information is lacking about the SHP in deep profiles, so we

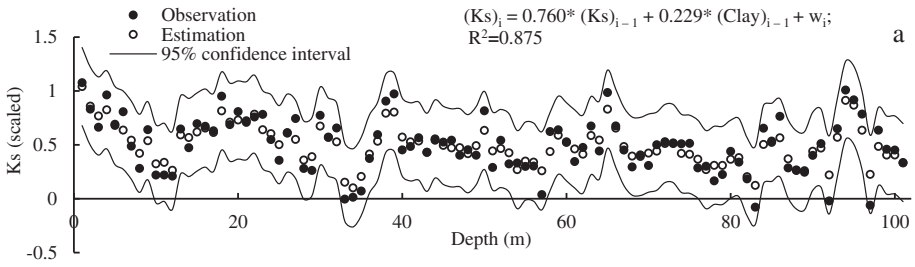

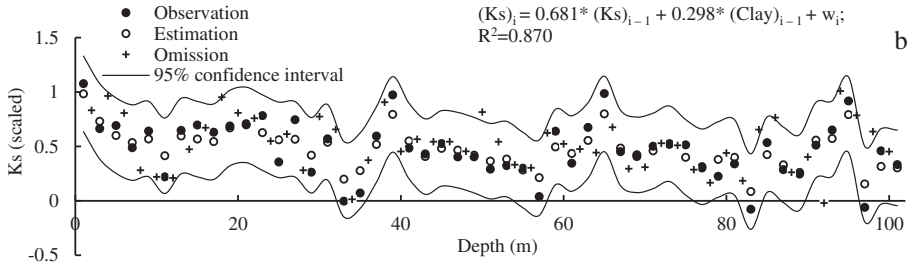

Fig. 5. State-space model of soil saturated hydraulic conductivity (Ks) and clay content using all measured Ks data (a) and 50% of the measured Ks data (b). Data were scaled using Eq. (4).

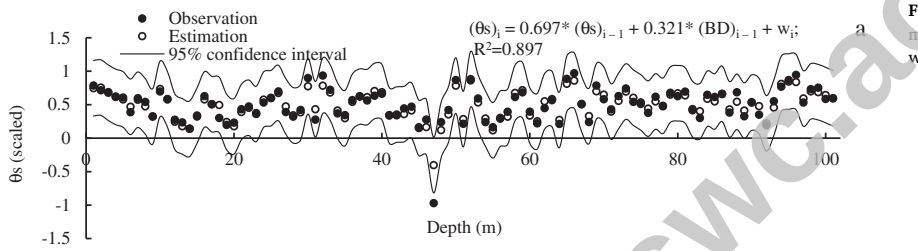

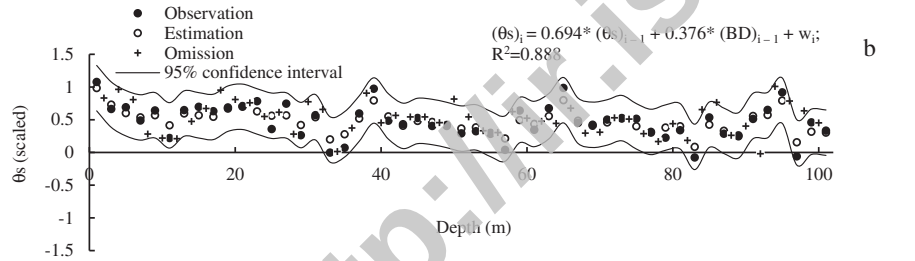

Fig. 6. State-space model of θs and bulk density (BD) using all measured θs data (a) and 50% of the measured θs data (b). Data were scaled using Eq. (4).

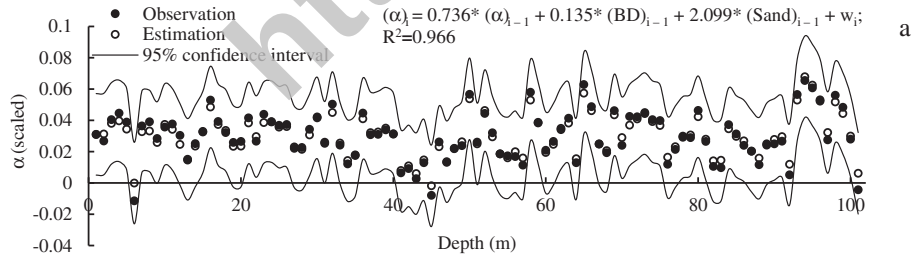

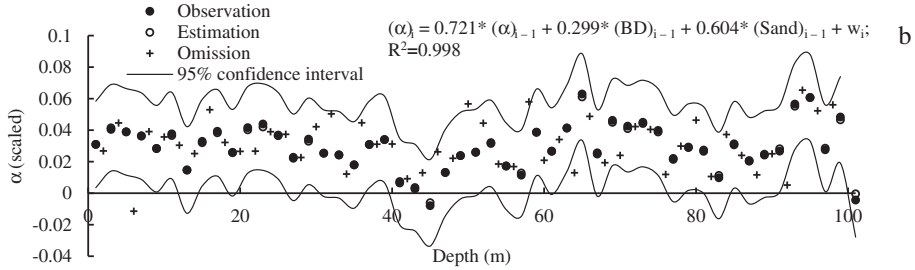

Fig. 7. State-space model of α, bulk density (BD) and sand content using all measured α data (a) and 50% of the measured α data (b). Data were scaled using Eq. (4).

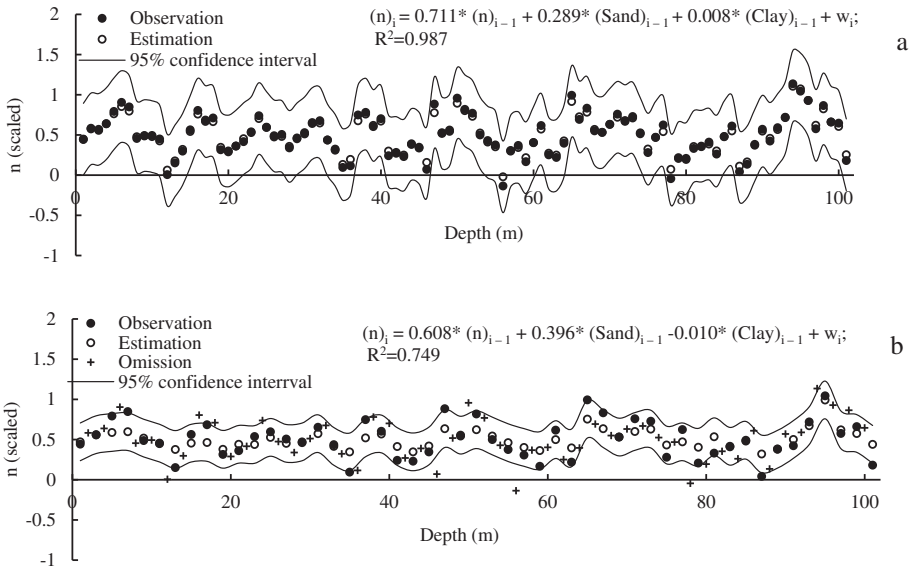

Fig. 8. State-space model of n, sand content and clay content using all measured n data (a) and 50% of the measured n data (b). Data were scaled using Eq. (4).

Table 4
Linear regression analysis of soil hydraulic properties (SHP) using the bulk density (BD), and sand and clay contents.

Linear regression model	R^2
Ks = 8.171 − 7.354 ∗ BD	0.276
Ks = − 4.105 + 0.083 – sand	0.090
Ks = − 1.397 − 0.085 ∗ clay	0.115
Ks = 6.849 − 6.726 ∗ BD + 0.055 ∗ sand	0.312
Ks = 8.296 − 6.53 ∗ BD − 0.055 ∗ clay	0.318
Ks = − 2.086 − 0.65 ∗ clay + 0.028 ∗ sand	0.110
Ks = 7.684 − 6.512 ∗ BD + 0.024 ∗ sand − 0.038 ∗ clay	0.314
θs = 0.796 − 0.234 ∗ BD	0.490
θs = 0.405 + 0.003 ∗ sand	0.165
θs = 0.488 − 0.003 ∗ clay	0.187
θs = 0.753 − 0.214 ∗ BD + 0.002 ∗ sand	0.560
θs = 0.799 − 0.210 ∗ BD − 0.002 ∗ clay	0.557
θs = 0.459 + 0.001 ∗ sand − 0.002 ∗ clay	0.193
θs = 0.772 − 0.209 ∗ BD + 0.001 ∗ sand − 0.001 ∗ clay	0.564
α = 0.346 − 1.891 ∗ BD	0.283
α = − 2.849 + 0.028 ∗ sand	0.169
α = − 2.102 − 0.022 ∗ clay	0.122
α = − 0.165 − 1.648 ∗ BD + 0.021 ∗ sand	0.375
α = 0.379 − 1.672 ∗ BD − 0.015 ∗ clay	0.330
α = − 2.673 + 0.023 ∗ sand − 0.006 ∗ clay	0.164
α = − 0.19 − 1.655 ∗ BD + 0.022 ∗ sand + 0.001 ∗ clay	0.368
n = 9.509 − 5.924 ∗ BD	0.170
n = − 0.673 + 0.118 ∗ sand	0.186
n = 2.74 − 0.104 ∗ clay	0.171
n = 7.158 − 4.808 ∗ BD + 0.098 ∗ sand	0.292
n = 9.697 − 4.687 ∗ BD − 0.083 ∗ clay	0.269
n = 0.9 + 0.075 ∗ sand − 0.051 ∗ clay	0.195
n = 7.848 − 4.631 ∗ BD + 0.072 ∗ sand − 0.031 ∗ clay	0.291

investigated the spatial distributions of the SHP, and estimated the relationships between SHP and soil properties in a 100-m profile using state-space modeling. The results showed that due to the unique profile structure of the Loess Plateau, spatial autocorrelations were not high for the SHP. BD was shown to be an important variable in terms of its contributions to the variations in all the SHP. The soil physical properties (BD, sand, and clay) explained variations in the SHP, but SOC made no contribution among the soil chemical properties. In addition, the performance of the models was similar or even better when using 50% of the data. Compared with the results obtained by multiple regression analysis, state-space analysis described the relationships between the SHP and other variables better, thereby indicating that state-space modeling is a more effective tool for estimating the relationships among soil variables. Our study provides important parameters for numerical simulations of soil water dynamics in deep soil layers, which are important for predicting SHP based on the available soil physical data.

Acknowledgements

This study was supported by the National Natural Science Foundation of China for a major international cooperation program between China and England (41571130081), the National Natural Science Foundation of China (41371242 and 41530854), and the Key Deployment Project of the Chinese Academy (KFZD-SW-306). The authors thank the editor and reviewers for their valuable comments and suggestions.

References

Bevington, J., Piragnolo, D., Teatini, P., Vellidis, G., Morari, F., 2016. On the spatial variability of soil hydraulic properties in a Holocene coastal farmland. Geoderma 262, 294–305.
Biswas, A., Si, B.C., 2009. Spatial relationship between soil hydraulic and soil physical properties in a farm field. Can. J. Soil Sci. 89, 473–488.
Buttle, J., House, D., 1997. Spatial variability of saturated hydraulic conductivity in shallow macroporous soils in a forested basin. J. Hydrol. 203, 127–142.
Ding, Z., Liu, D., Liu, X., Chen, M., An, Z., 1989. Climate cycle of 37 times since 2.5 million. Chin. Sci. Bull. 34, 1494–1496.
Duan, L., Huang, M., Zhang, L., 2016. Use of a state-space approach to predict soil water storage at the hillslope scale on the Loess Plateau, China. Catena 137, 563–571.
Fu, T., Chen, H., Zhang, W., Nie, Y., Wang, K., 2015. Vertical distribution of soil saturated hydraulic conductivity and its influencing factors in a small karst catchment in Southwest China. Environ. Monit. Assess. 187, 1–11.
Genuchten, M.T.V., 1980. A closed-form equation for predicting the hydraulic conductivity of unsaturated soils. Soil Sci. Soc. Am. J. 44, 892–898.
Goovaerts, P., 1999. Geostatistics in soil science: state-of-the-art and perspectives. Geoderma 89, 1–45.
Horn, R., 2004. Time dependence of soil mechanical properties and pore functions for arable soils. Soil Sci. Soc. Am. J. 68, 1131–1137.
Jia, X., Shao, M., Wei, X., Horton, R., Li, X., 2011. Estimating total net primary productivity of managed grasslands by a state-space modeling approach in a small catchment on the Loess Plateau, China. Geoderma 160, 281–291.
Jia, X., Shao, M.A., Wei, X., 2012. State-space prediction of soil respiration time series in temperate, semi-arid grassland in northern China. Soil Res. 50, 293–303.
Kai-Hua, L., Shao-Hui, X., Ji-Chun, W., Shu-Hua, J., Qing, L., 2011. Assessing soil water retention characteristics and their spatial variability using pedotransfer functions. Pedosphere 21, 413–422.
Kalman, R.E., 1960. A new approach to linear filtering and prediction problems. J. Basic Eng. 82, 35–45.
Lai, J., Ren, L., 2016. Estimation of effective hydraulic parameters in heterogeneous soils at field scale. Geoderma 264, 28–41.
Lin, H., 2010. Earth's critical zone and hydropedology: concepts, characteristics, and advances. Hydrol. Earth Syst. Sci. 6, 3417–3481.

Liu, Y.P., Tong, J., Li, X.N., 2005. Analysing the silt particles with the Malvern Mastersizer 2000. Water Conserv. Sci. Technol. Econ. 11, 329–331.
Liu, Z., Shu, Q., Wang, Z., 2007. Applying pedo-transfer functions to simulate spatial heterogeneity of cinnamon soil water retention characteristics in Western Liaoning Province. Water Resour. Manag. 21, 1751–1762.
Liu, Z., Shao, M.A., Wang, Y., 2012. Estimating soil organic carbon across a large-scale region: a state-space modeling approach. Soil Sci. 177, 607–618.
Lu, D., Shao, M., Horton, R., Liu, C., 2004. Effect of changing bulk density during water desorption measurement on soil hydraulic properties. Soil Sci. 169, 319–329.
Mallants, D., Mohanty, B.P., Jacques, D., Feyen, J., 1996. Spatial variability of hydraulic properties in a multi-layered soil profile. Soil Sci. 161, 167–181.
Mallants, D., Mohanty, B.P., Vervoort, A., Feyen, J., 1997. Spatial analysis of saturated hydraulic conductivity in a soil with macropores. Soil Technol. 10, 115–131.
National Research Council, 2001. Basic Research Opportunities in Earth Science. National Academy Press, Washington DC.
Nelson, D.W., Sommers, L.E., 1982. Total carbon, organic carbon and organic matter, in Methods of Soil Analysis (Part 2, 2nd Ed.). Agronomy Monograph. 9. ASA and SSSA, Madison, WI, pp. 534–580.
Nielsen, D.R., Bouma, J., 1985. Soil spatial variability. In: Proceedings of a Workshop of the ISSS and the SSSA, Las Vegas, USA, 30 November–1 December, 1984. Pudoc.
Nielsen, D.R., Wendroth, O., Pierce, F.J, 1999. Emerging concepts for solving the enigma of precision farming research. In: Robert, P.C., Rust, R.H., Larson, W.E. (Eds.), Proceedings of Fourth International Conference on Precision Agriculture. Minneapolis, MI, pp. 303–318.
She, D., Gao, X., Song, J., Timm, L.C., Hu, W., 2014. Soil organic carbon estimation with topographic properties in artificial grassland using a state-space modeling approach. Can. J. Soil Sci. 94, 503–514.
She, D., Chen, Q., Timm, L.C., Beskow, S., Hu, W., Caldeira, T.L., Oliveira, L.M.D., 2017. Multi-scale correlations between soil hydraulic properties and associated factors along a Brazilian watershed transect. Geoderma. 286, 15–24.
Shumway, R.H., 1988. Applied statistical time series analysis (Prentice Hall series in statistics). Technometrics 1, 353–354.
Shumway, R.H., Stoffer, D.S., 1982. An approach to time series smoothing and forecasting using the EM algorithm. J. Time Ser. Anal. 3, 253–264.
Shumway, R.H., Biggar, J.W., Morkoc, F., Bazza, M., Nielsen, D.R., 1989. Time and frequency domain analysis of field observations. Soil Sci. 147, 1344–1354.
Sobieraj, J., Elsenbeer, H., Coelho, R., Newton, B., 2002. Spatial variability of soil hydraulic conductivity along a tropical rainforest catena. Geoderma 108, 79–90.
Strock, J., Cassel, D., Gumpertz, M., 2001. Spatial variability of water and bromide transport through variably saturated soil blocks. Soil Sci. Soc. Am. J. 65, 1607–1617.
Strudley, M.W., Green, T.R., Ascough, J.C., 2008. Tillage effects on soil hydraulic properties in space and time: state of the science. Soil Tillage Res. 99, 4–48.
Timm, L., Reichardt, K., Cassaro, F., Tominaga, T., Bacchi, O., Oliveira, J., Dourado-Neto, D., 2003. State-space approach for evaluating the soil–plant–atmosphere system. Lectures Given at the College on Soil Physics Trieste. pp. 3–21.
Timm, L., Reichardt, K., Oliveira, J., Cassaro, F., Tominaga, T., Bacchi, O., Dourado-Neto, D., Nielsen, D., 2004. State-space approach to evaluate the relation between soil physical and chemical properties. R. Bras. Ci. Solo 28, 49–58.
Wang, L., Wang, Q., Wei, S., Shao, M.A., Li, Y., 2008. Soil desiccation for Loess soils on natural and regrown areas. For. Ecol. Manag. 255, 2467–2477.
Wang, Y., Shao, M.a., Han, X., Liu, Z., 2015. Spatial variability of soil parameters of the van Genuchten model at a regional scale. CLEAN–Soil Air Water 43, 271–278.
Wendroth, O., Rogasik, H., Koszinski, S., Ritsema, C., Dekker, L., Nielsen, D., 1999. State–space prediction of field–scale soil water content time series in a sandy loam. Soil Tillage Res. 50, 85–93.
Wendroth, O., Jürschik, P., Kersebaum, K.C., Reuter, H., Kessel, C.V., Nielsen, D.R., 2001. Identifying, understanding, and describing spatial processes in agricultural landscapes—four case studies. Soil Tillage Res. 58, 113–127.
Wendroth, O., Reuter, H.I., Kersebaum, K.C., 2003. Predicting yield of barley across a landscape: a state-space modeling approach. J. Hydrol. 272, 250–263.
Zhao, C., Shao, M., Jia, X., 2014. Distribution and simulation of saturated soil hydraulic conductivity at a slope of northern Loess Plateau. Adv. Water Sci. 25, 806–815.